TABLE A2. DISPERSION COEFFICIENTS FOR MODELS III AND IV

Model III		Model IV	
$u_{(n)}$ (cm/s) × 60	$D_{(n)}$ (cm²/s) × 60	$u_{(n)}$ (cm/s) × 60	$D_{(n)}$ (cm²/s) × 60
0.739	0.0177	0.877	0.139
0.350	0.00800	0.550	0.0920
0.908	0.0224	1.20	0.199
0.154	0.00297	0.350	0.0625
1.24	0.0360	0.151	0.0291
0.901	0.0234	0.548	0.0899

TABLE A3. DISPERSION COEFFICIENTS FOR MODELS V AND VI

Model V		Model VI	
$u_{(n)}$ (cm/s) × 60	$D_{(n)}$ (cm²/s) × 60	$u_{(n)}$ (cm/s) × 60	$D_{(n)}$ (cm²/s) × 60
0.721	0.446	0.874	0.0705
0.877	0.640	0.550	0.0533
0.156	0.0732	0.357	0.0264
0.358	0.176	0.155	0.0152
1.21	0.826	1.20	0.0799
0.565	0.363	0.560	0.0551
0.362	0.185	0.739	0.0613

TABLE A4. DISPERSION COEFFICIENTS FOR MODELS VII AND VIII

Model VII		Model VIII	
$u_{(n)}$ (cm/s) × 60	$D_{(n)}$ (cm²/s) × 60	$u_{(n)}$ (cm/s) × 60	$D_{(n)}$ (cm²/s) × 60
0.819	0.0249	0.902	0.277
1.20	0.0309	0.566	0.106
0.548	0.0110	0.155	0.0359
0.351	0.00936	0.360	0.053
0.157	0.00304		
0.565	0.0155		

ACKNOWLEDGMENT

Part of the material in this paper was presented at the 1976 New York Meeting of the American Chemical Society. We express our thanks to the American Chemical Society for permission to publish this material.

Manuscript received March 28, 1977; revision received July 5, and accepted July 8, 1977.

Stochastic Models of Algal Photosynthesis in Turbulent Channel Flow

MAYUR SHETH

and

DORAISWAMI RAMKRISHNA

Department of Chemical Engineering
Indian Institute of Technology
Kanpur, U.P. 208016, India

and

ARNOLD G. FREDRICKSON

Department of Chemical Engineering
& Materials Science
University of Minnesota
Minneapolis, Minnesota 55455

Models have been formulated and analyzed for photosynthesis by algae in turbulent, channel flow. Analytical and computational results for different stochastic, kinematic models of algal motion have been obtained for two different rate mechanisms. The results indicate that turbulent mixing can achieve an increase in the rates and efficiencies of photosynthesis by realizing the intermittency effects. Optimum levels of turbulence are shown to exist in turbulent channel flow for the mass cultivation of algae. The methodology of this paper is relevant to photochemical reactions in general.

SCOPE

Mass cultures of algae have been of interest to engineers as a possible supplemental protein source; for the production of enzymes, vitamins, and other biochemicals; as nitrogen fixers in fields for agricultural cultivation; as photosynthetic gas exchangers in life-support systems; etc. An essential feature of algal growth is the photosynthetic activity of the cells which converts carbondioxide and water with the aid of absorbed visible radiation into cellular material and oxygen. There are two aspects of algal photosynthesis which are important to the mass cultivation of algae. First, the photosynthetic rate increases with the amount of light intensity but eventually tapers off to a maximum value. Second, photosynthesis involves light and dark reactions in sequence so that a suitable flashing light pattern may increase the efficiency of light utilization measured by the photosynthetic yield relative to the energy consumed by the culture. Since algal cultures must of necessity be dense to provide for adequate absorption of light, cells removed from the surface exposed to light would receive relatively less radiation than those at the surface. If cells in the interior must receive adequate radiation, those at the surface would have to receive more than they need. Thus a compromise must be struck between low efficiency of energy utilization at the surface and low photosynthetic rates in the interior of the culture.

In view of the advantages which may accrue from suitable intermittent light patterns, the question has been raised as to whether naturally occurring turbulence in various flow situations would serve the purpose of exposing cells in the interior to better lighting conditions and

Correspondence concerning this paper should be addressed to D. Ramkrishna, School of Chemical Engineering, Purdue University, West Lafayette, Indiana 47907.

to transport cells between regions of varying light intensity in a suitably intermittent manner.

Turbulent channel flow, which offers an attractive prospect for mass cultivation of algae, is the subject of this work. Models are proposed for the kinematics of algal motion in turbulent channel flow, which vary in detail from one which uses purely random motion described by white noise to one which incorporates available hydrodynamic information about turbulent channel flow. The advantage of white noise lies in the analytical tractability of the models based on it, although this gain must be weighed with the expense of realism. The more realistic models do not submit to analytical treatment so that suitable Monte Carlo simulation methods based on appropriate numerical algorithms provide the sole route to quantitative assessment of such models. In this work, the Fokker-Planck equation (which is satisfied by the probability density of the solution process) is solved analytically to evaluate the white noise model, and an algorithm due to Rao et al. has been used to solve the more complicated models based on turbulent hydrodynamics. Photosynthetic rates for turbulent flow have been evaluated and compared with those for stagnant cultures.

In comparing photosynthetic rates and efficiencies of energy utilization, quantities both at the microscopic and macroscopic levels have been used. The microscopic quantity represents the time averaged value for a cell with a stated average position in the culture, and the macroscopic quantity is the space averaged value of the microscopic quantity.

CONCLUSIONS AND SIGNIFICANCE

The kinematics of algal motion in turbulent channel flow has been modeled based on the assumption of negligible inertia in various ways differing in the degree of detail. All the models predict an improved rate of photosynthesis in turbulent flow over those in stagnant cultures or in streamlined flow with no transverse mixing. The level of improvement depends critically on the light intensity and the culture density.

The microscopic photosynthetic rate and efficiency of energy utilization is critically dependent on not only the light intensity and the culture density but also on the mean position of the cell with respect to the illuminated surface. Thus, lower light intensities, higher culture densities, and distance from the surface up to a limit all enhance the photosynthetic rate and efficiency. This enhancement ranges from marginal to a nearly twofold increase over those in flows without transverse mixing. In some cases, where cells are close to the surface, there is a drop in photosynthetic rate. Whether or not there is an improvement in the macroscopic photosynthetic rate and efficiency of energy utilization depends on the culture density, light intensity, and depth of the channel. The white noise model predicts over a 50% enhancement of the macroscopic rate, efficiency, and productivity, indicating the merits of increased turbulence. The more detailed models relate the microscopic photosynthetic rate to Reynolds number and determine situations under which improved rates are obtained. Although the macroscopic rates could not be explicitly computed for these models, calculations of microscopic rates indicate sizable increase in photosynthetic rate.

Thus mass culturing of algae in channels under turbulent flow conditions appears to be an attractive prospect. The methodology in this paper is particularly useful for photochemical reactions in general.

PREVIOUS WORK

Fredrickson and Tsuchiya (1970) have provided a comprehensive review of the various aspects of algal photosynthesis, such as kinetics, light intermittency effects, and about different experimental and mathematical work directed towards the cultivation of algae under different flow conditions. It is therefore not necessary to discuss them here in any detail. It is fair to conclude that the advantages of turbulence in improving photosynthetic rates and efficiencies of utilization of light energy have been subject to conflicting verdicts by different workers. Of course, some of these could have arisen because of a difference in flow configurations and dimensions of equipment, both of which could profoundly affect the results.

Powell et al. (1965) have analyzed the effect of turbulence in a flat channel, illuminated from both sides. The motion of algae was modeled as a ten-state Markov process, in which as a cell moves a step forward there is a probability that it may also move up or down. The Markov-transition probability matrix was calculated by correlating it to Prandtl's mixing length theory of turbulent momentum transport. Powell et al. (1965) found that optimum transit time could be found from light to dark but with too large a variance. Thus, cells may commute between light and dark regions too frequently, which led to their suggestion that turbulence was unsuitable. However, they did not calculate the rates and efficiencies of photosynthesis. We contend that it is unrealistic to expect that any given turbulent flow would yield a preconceived optimum intermittent light pattern and that the effectiveness of turbulence in improving photosynthetic rates can only be determined by a direct calculation. Gordon (1972) used an approach similar to that of Powell et al. (1965) and predicted increased efficiencies of photosynthesis. However, Gordon did not relate the stochastic matrix to hydrodynamic parameters.

Fredrickson, Brown, Miller, and Tsuchiya (1961) used the kinetic expression of Lumry and Rieske to obtain analytic expressions for the efficiency of photosynthesis in a rectangular growth chamber. They considered two extreme cases; one was an unstirred culture and the other was a perfectly stirred culture. In the first case, each cell carries out photosynthesis at the rate corresponding to the local intensity. In the second, the mixing is assumed to be so vigorous that all the cells carry out photosynthesis at the space averaged light intensity. The rates in the well-stirred case were found to be much higher, although no particular increase in efficiency was noted. Of course, the intermittency effect is not accounted for in the work of Fredrickson et al., but it does point to the advantages of mixing.

In the present work, algal photosynthesis is analyzed in turbulent channel flow using the kinetic expression de-

veloped by Lumry and Rieske (1959) and that due to Tamiya (1949), which are presented below. The overall reaction of photosynthesis is

$$n\,CO_2 + n\,H_2O \xrightarrow{h\nu} [CH_2O]_n + n\,O_2$$

chlorophyll enzymes, etc. — cellular material

Lumry and Rieske (1959) proposed the following mechanism:

$$T \xrightarrow{k_L I} T^* \qquad \text{(Light reaction)}$$

$$H_2O + T^* \xrightarrow{k_D} T + H + OH \qquad \text{(Dark reaction)}$$

$$H + \text{Oxidant} \rightarrow \text{Reduced oxidant} \rightarrow \text{Products} \quad \text{(Fast)}$$

$$4\,OH \rightarrow O_2 + 2\,H_2O \quad \text{(Fast)}$$

In the above scheme, T represents the trapping centers for excitation energy $h\nu$. These trapping centers are pigment molecules such as chlorophylls, enzymes, etc. The rate of photosynthesis, R_p, is given by $k_D[T^*]$, where $[T^*]$ is the concentration of successful trapping centers, which satisfies the differential equation

$$\frac{d}{dt}[T^*] = k_L I[T] - k_D[T^*]$$

$$= k_L I\{[T]_o - [T^*]\} - k_D[T^*] \quad (1)$$

Tamiya (1949) gives a somewhat more detailed mechanism:

$$S \xrightarrow{k_s I} S'$$

$$S' + E_1 \xrightarrow{k_1} S + E_2$$

$$E_2 \xrightarrow{k_2} E_1 + \text{Products}$$

$$S' + S' \xrightarrow{k_{ss}} 2S$$

where S represents the photosynthetic sensitizers such as chlorophylls, carotenoids, etc.; E_1 are enzymatic components which accept the excitation energy from activated sensitizers S' to form E_2. The sums $[S] + [S'] \equiv C$ and $[E_1] + [E_2] \equiv \epsilon$ are assumed constant in the cell. The rate of photosynthesis is given by $k_2[E_2]$, where $[E_2]$ derives from the solution of the equations

$$\frac{d[S']}{dt} = k_s I\{C - [S']\} - k_1[S']\{\epsilon - [E_2]\} - 2k_{ss}[S']^2 \quad (2)$$

$$\frac{d[E_2]}{dt} = k_1[S']\{\epsilon - [E_2]\} - k_2[E_2] \quad (3)$$

Both mechanisms account for the saturating influence of light on photosynthetic rate and the sequential nature of light and dark reactions so that they can predict the intermittency effects referred to earlier.

STOCHASTIC MODELS OF ALGAL MOTION IN CHANNEL FLOW

For a uniform light intensity on the top surface of the channel, the light intensity in the interior of the flow can be calculated as a deterministic function of position using Lambert-Beer's law. Thus, for distance z measured from the channel surface into the flow, we may write the local intensity as

$$I(z) = I_o \exp(-\beta\rho z) \quad (4)$$

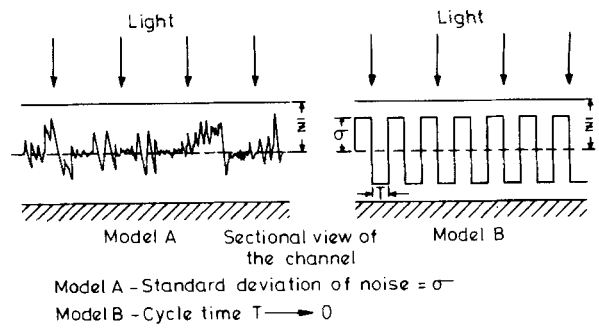

Fig. 1. The models for the motion of an algal cell in turbulent channel flow.

Since the light intensity is a function of vertical distance alone from the illuminated channel surface, it is only the z coordinate of the cell that is of direct interest to us. In steady, turbulent channel flow it is well known that the time smoothed vertical component of velocity is zero. If the algae are presumed to possess negligible inertia, then the kinematic equation

$$\frac{dZ}{dt} = v_z = v_z' \quad (5)$$

where v_z' is the velocity fluctuation, implies that

$$\frac{d\overline{Z}}{dt} = \overline{v_z'} = 0 \quad (6)$$

in which the overbars signify the time smoothing operation. Equation (6) shows that the average position of any given cell does not vary with time.

We will consider various models of increasing detail for the algal trajectory. In all models, however, we remain oblivious to the x and y coordinates of the cell; insofar as v_z' may be statistically correlated to v_x' and v_y', some inexactness has been permitted by this procedure.

If we write

$$Z(t) = \overline{Z} + Z'(t) \quad (7)$$

then, from Equation (5), we must have

$$Z'(t) = \int_0^t v_z'\,dt' \quad (8)$$

The light intensity seen by a cell at $Z(t)$ is clearly

$$I[Z(t)] = I_o \exp\{-\beta\rho[\overline{Z} + Z'(t)]\} \quad (9)$$

To calculate the instantaneous photosynthetic rate, (9) must be inserted in Equation (1), if the Lumry-Rieske mechanism is of interest, or into Equation (2), if Tamiya's mechanism is to be used.

We will be concerned with models for $Z'(t)$ either directly or through modeling of v_z' [see Equation (8)]. Before proceeding, we observe that the time smoothed macroscopic photosynthetic rate may be calculated by integrating the time smoothed microscopic rate at various mean positions $\overline{z}$ and integrating over the channel width.

We first consider two very idealized models referred to as A and B. Model A assumes that

$$Z'(t) = \xi(t) \quad (10)$$

where $\xi(t)$ is white, Gaussian noise with the properties

$$E[\xi(t)] = 0 \quad E[\xi(t)\ \xi(t+\tau)] = \sigma^2\delta(\tau) \quad (11)$$

We refer to Wong (1971) for more details. Equation (11) shows that $\xi(t)$ is an uncorrelated random process. For any fixed t, ξ has a Gaussian distribution with zero mean and variance σ^2.

Model B pictures the motion of an algal cell as consisting of small deviations σ on either side of the mean path as shown in Figure 1. These deviations are to be very small to approximate turbulent flow conditions at least crudely. As against the premise of model A, model B views the motion of the cell as totally correlated.

Clearly, both models A and B are very unrealistic. There is no random process v_z' that will yield white noise through Equation (8). Also, turbulent flow cannot be totally correlated as in model B. What makes the analysis of models A and B worthwhile is that turbulent flow must be somewhere between uncorrelated and correlated motion. Thus, the predictions of these two models could establish limits within which the true results must lie. Furthermore, models A and B can be handled analytically without numerical methods for solving the stochastic differential equations. We discuss only the methods for model A. Model B is handled by an entirely different technique called the relaxed variational analysis due to Warga (1961), which is an effective technique for dealing with the behavior of dynamical systems under the influence of rapidly switching controls. We will not go into this technique here but will present the results of calculations made on model B.

The Lumry-Rieske kinetics for photosynthesis has been used for both models A and B.

MODEL A

This model can be neatly handled by analytical means if the light intensity (9) can be linearized in a statistical sense identical to that used by Pell and Aris (1969).* Thus, we write

$$I[Z(t)] = \bar{I}(\bar{Z}, \sigma^2) + \xi'(t) \tag{12}$$

where $\xi'(t)$, although only approximately Gaussian, may be regarded as Gaussian, white noise with zero mean and variance to be identified presently. The mean value $\bar{I}(\bar{Z}, \sigma^2)$ of I is given by

$$\bar{I}(\bar{Z}, \sigma^2) = E\{I_o \exp[-\beta\rho(\bar{Z} + \xi)]\}$$

$$= \int_{-\infty}^{\infty} I_o \exp - [\beta\rho(\bar{Z} + \xi)] \frac{e^{-\frac{1}{2}\frac{\xi^2}{\sigma^2}}}{\sqrt{2\xi}\,\sigma} d\xi$$

$$= I(\bar{Z}) \exp\left(\frac{\beta\rho\sigma^2}{2}\right) \tag{13}$$

The variance of $\xi'(t)$ is now computed from

$$E[\xi'(t)^2] = E\{I[Z(t)] - \bar{I}(\bar{Z}, \sigma^2)\}^2 = 2D_1$$

where

$$2D_1 = I^2(\bar{Z})\,[\exp(2\beta^2\rho^2\sigma^2) - \exp(\beta^2\rho^2\sigma^2)] \tag{14}$$

Equation (1) may now be rewritten, using (12) and (13), to obtain, in dimensionless form

$$\frac{dx}{dt} = k_L \bar{I}(\bar{Z}, \sigma^2)(1 - x) - k_D x + k_L(1 - x)\xi'(t) \tag{15}$$

Equation (15) is a stochastic differential equation or the Langevin equation, which has been the subject of considerable discussion (Mortensen, 1969; Wong, 1971; Rao et al., 1974*a*) with respect to its alternative but not equivalent form called the Ito form:

$$x(t) = x(0) + \int_o^t [k_L \bar{I}(\bar{Z}, \sigma^2)(1 - x) - k_D x]dt'$$

$$+ \int_o^t k_L(1 - x)\sqrt{2D_1}\, dW(t') \tag{16}$$

Here $dW(t)$ is called the standard Wiener process with zero mean and unit variance. We will not dwell on the intricacies of the relationship between (15) and (16) here but will recognize their differences by calling (15) the white noise model and (16) the Ito model.

Now, the solution of either of Equations (15) and (16) is a Markov process whose time varying probability density satisfies a partial differential equation called the Fokker-Planck equation (see Wong, 1971). The Fokker-Planck Equation for (15) is given by

$$\frac{\partial}{\partial t} p(x, t, \mid x_o, t_o) =$$

$$-\frac{\partial}{\partial x}\{[k_L \bar{I}(\bar{Z}, \sigma^2)(1 - x) - k_D x$$

$$- k_L^2 D_1(1 - x)]\, p(x, t \mid x_o t_o)\}$$

$$+ \frac{1}{2}\frac{\partial^2}{\partial x^2}[k_L^2(1 - x)^2\, 2D_1\, p(x, t, \mid x_o, t_o)] \tag{17}$$

while Equation (16) has the Fokker-Planck equation

$$\frac{\partial}{\partial t} p(x, t \mid x_o, t_o) =$$

$$-\frac{\partial}{\partial x}\{[k_L \bar{I}(\bar{Z}, \sigma^2)(1 - x) - k_D x]\, p(x, t \mid x_o, t_o)\}$$

$$+ \frac{1}{2}\frac{\partial^2}{\partial x^2}[k_L^2(1 - x)^2\, 2D_1\, p(x, t \mid x_o, t_o)] \tag{18}$$

Equations (17) and (18) differ in the first term on the right-hand side that brings out the nonequivalence of Equations (15) and (16). From either equation, the expected or average value of x, denoted M_x, is obtained by taking the first moment of the equation. Thus, for the white noise model, one obtains

$$\frac{dM_x}{dt} = k_1 \bar{I}(\bar{Z}, \sigma^2) - [k_L \bar{I}(\bar{Z}, \sigma^2) + k_D] M_x$$

$$- k_L^2 D_1 - k_L^2 D_1 M_x \tag{19}$$

with a steady state value

$$M_{x,s} = \frac{k_L[\bar{I}(\bar{Z}, \sigma^2) - k_L D_1]}{k_L[\bar{I}(\bar{Z}, \sigma^2) - k_L D_1] + k_D} \tag{20}$$

The Ito model, on the other hand, gives

$$\frac{dM_x}{dt} = k_L \bar{I}(\bar{Z}, \sigma^2)(1 - M_x) - k_D M_x \tag{21}$$

which has a steady state value

$$M_{x,s} = \frac{k_L \bar{I}(\bar{Z}, \sigma^2)}{k_L \bar{I}(\bar{Z}, \sigma^2) + k_D} \tag{22}$$

We have dwelt a bit on the parallel treatment of the white noise and Ito models because the reliability of such stochastic calculations has been burdened by the ambiguity pertaining to which of the interpretations [(15) or (16)] may apply to the physical problem. We are fortunate here not to have to resolve this question because the terms accounting for the difference between (20) and (22) are numerically negligible. The final implication is that the results of our calculations are free from irksome ambiguities. Figure 2 bears out this claim for the photosynthetic

* This linearization is unnecessary for model B so that it is not employed there.

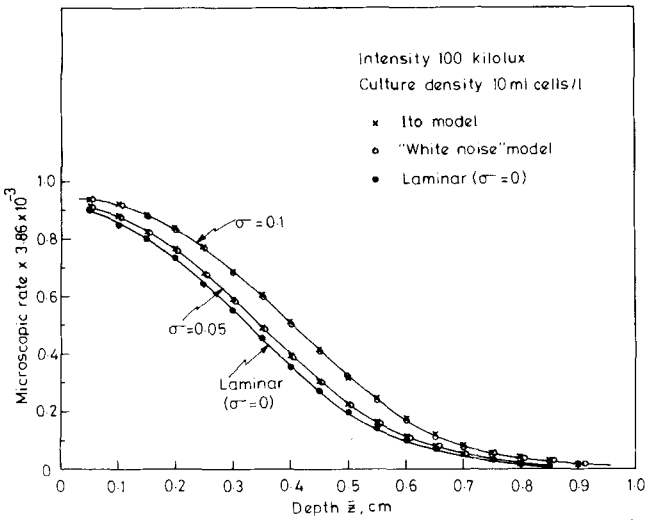

Fig. 2. Comparison of "white noise" and Ito models: microscopic rate as a function of depth.

rate calculated for different values of average depth $\overline{Z}$ from the formula

$$\overline{R}_m(\overline{Z}, \sigma^2) = k_D M_{x,s}$$

Since, in practice, the photosynthetic rate would actually fluctuate about the mean rate, we obtain the variance $V(\overline{Z}, \sigma^2)$ from

$$V(\overline{Z}, \sigma^2) = E[R(\overline{Z}, \sigma^2) - \overline{R}_m(\overline{Z}, \sigma^2)]^2$$
$$= k_D^2 [W_x(\overline{Z}, \sigma^2) - M_x^2]$$

where $W_x(\overline{Z}, \sigma^2)$, the second moment of $x(t)$, is found from the Fokker-Planck Equation (17) or (18). For (17) we obtain the steady state value

$$W_{x,s} = \frac{[k_L \overline{I}\,(\overline{Z}, \sigma^2) - 2k_L^2 D_1] M_{x,s} + k_L^2 D_1}{k_L \overline{I}\,(\overline{Z}, \sigma^2) + k_D - 2D_1} \quad (23)$$

The corresponding coefficient of variation of photosynthetic rate about the mean value, denoted $\overline{S}(\overline{Z}, \sigma^2)$, is given by

$$\overline{S}(\overline{Z}, \sigma^2) = \frac{\sqrt{V(Z, \sigma^2)}}{k_d M_{x,s}} \quad (24)$$

The preceding quantity is a relevant calculation because a large coefficient of variation about a slight enhancement of photosynthetic rate over that for laminar* flow would offset the advantage.

Now, the macroscopic photosynthetic rate is obtained by integrating $\overline{R}_m$ w.r.t. $\overline{Z}$. If oxygen consumption for respiration is accounted for, the net photosynthetic rate in terms of oxygen production is given by

$$\overline{R}(\sigma^2) = \frac{k_D}{\beta} \ln \frac{k_D + k_L I_o \exp\left(\frac{\beta^2\rho^2\sigma^2}{2}\right)}{k_L I_o \exp\left(\frac{\beta^2\rho^2\sigma^2}{2}\right) \exp(-\beta\rho L) + k_D} - k_{r\rho} \quad (25)$$

where $k_{r\rho}$ is the respirational rate. When σ is put equal to zero in (25), we have the result obtained by Fredrickson et al. (1961) for the unstirred case.

The efficiency of photosynthesis is given by

$$E = \frac{\overline{R}AL}{A I_o} = \frac{\overline{R}L}{I_o} \quad (26)$$

Since neither low rate and high efficiency of photosynthesis nor high rate and low efficiency are satisfactory, the productivity $P(\sigma^2)$ given by

$$P(\sigma^2) = \overline{R}(\sigma^2)\ E(\sigma^2) \quad (27)$$

is a more desirable quantity of comparison in evaluating photosynthesis in turbulent flow with respect to that in stagnant or laminar flow situations.

The values of rate constants and other parameters used in the calculations are presented in Table 1.

RESULTS FOR MODELS A AND B AND DISCUSSION

We present no details of model B which are present elsewhere (Sheth, 1974). The results are, however, shown in Figures 5 through 12.

Figure 2 shows the performance of model A in predicting the microscopic photosynthetic rate at various points

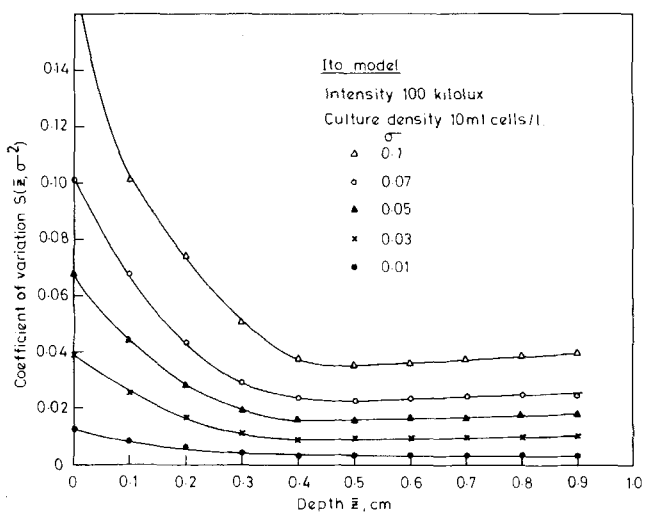

Fig. 3. Coefficient of variation as a function of depth.

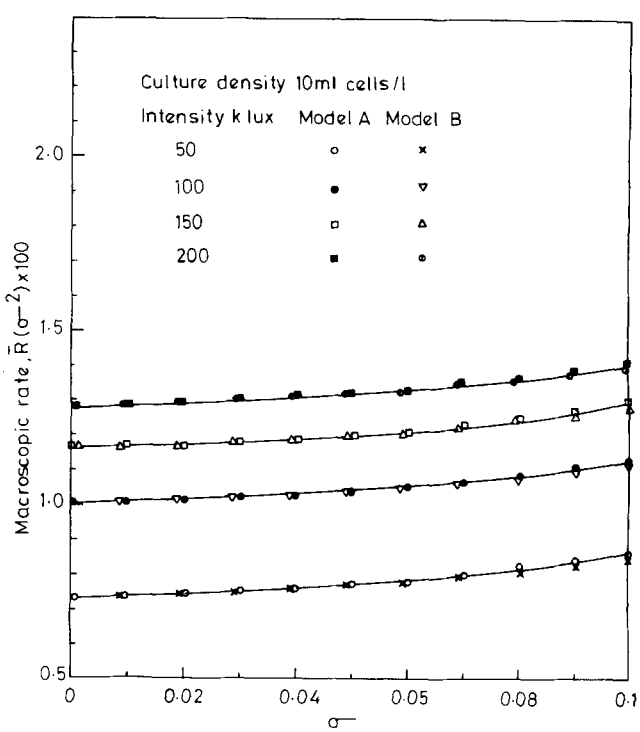

Fig. 4. Effect of noise parameter σ on macroscopic rate.

* By laminar flow here is meant a situation where cells do not receive transverse motion in the direction towards or away from light.

TABLE 1

k_L	k_D	k_r	β	L
0.52×10^{-3} g-mole O_2/hr-kilolux-ml cells	3.86×10^{-3} g-mole O_2/hr-ml cells	0.193×10^{-3} g-mole O_2/hr-ml cells	0.8 l/cm-ml cell	1 cm

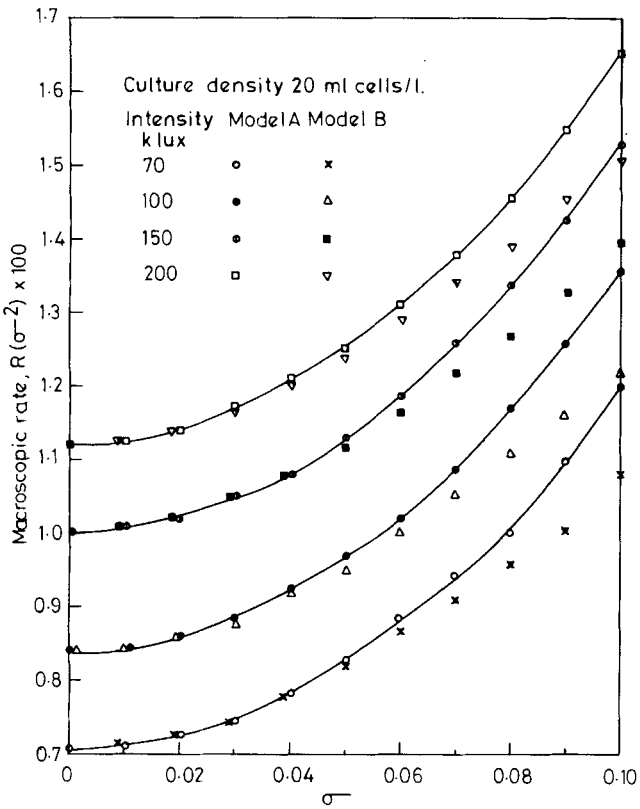

Fig. 5. Effect of noise parameter σ on macroscopic rate.

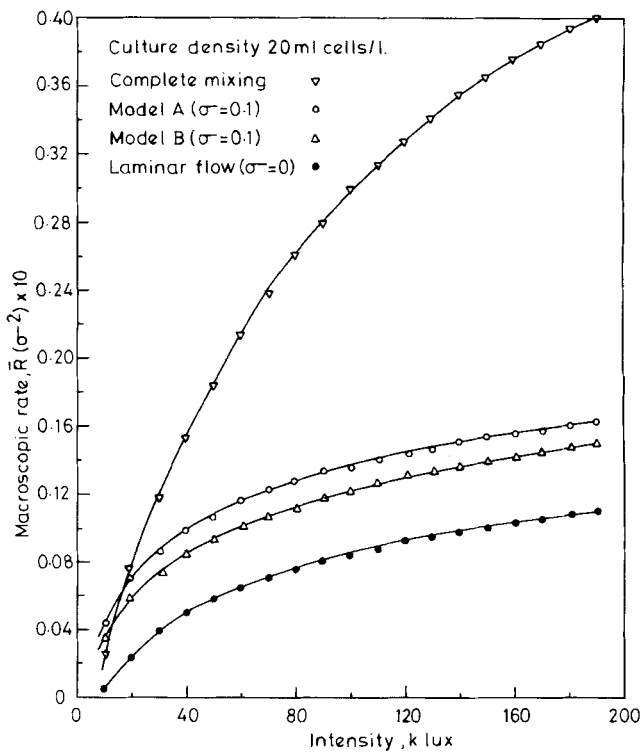

Fig. 6. Macroscopic rate as a function of light intensity.

in the channel. Higher levels of turbulence, implied by larger values of σ, are seen to improve the photosynthetic rate at all positions in the channel. The coefficient of variation about the average photosynthetic rate [see Equation (24)] appears in Figure 3 as a function of channel depth. The variations increase near the channel surface because of large light intensity gradients near the surface; this effect is even larger for higher culture densities. For the most part, it can be seen that the improvement in photosynthetic rate is well above the variation about the average value.

The macroscopic rate of photosynthesis is shown in Figure 4 for both models A and B as a function of the standard deviation about mean cell positions in the channel at various light intensities. Models A and B predict almost identical results. Figure 5 shows the situation at a higher culture density. From Figures 4 and 5, it is seen that for increasing values of σ, both models A and B show an increase in the photosynthetic rate. This increase is significantly higher at higher culture densities, which is in agreement with the conditions stated by Kok (1953).

An important further point to be noted from Figure 5 is that for equal values of σ, model A predicts a greater increase in rate, apparently contradicting a popular view that rapid periodic motion of an algal cell is superior to purely random motion in bringing about the intermittency effects. However, it should be realized that the random motion may subject the algal cells to deviations much greater than σ; even if the probability of such deviations is small, they expose the cells to very high light intensities near the

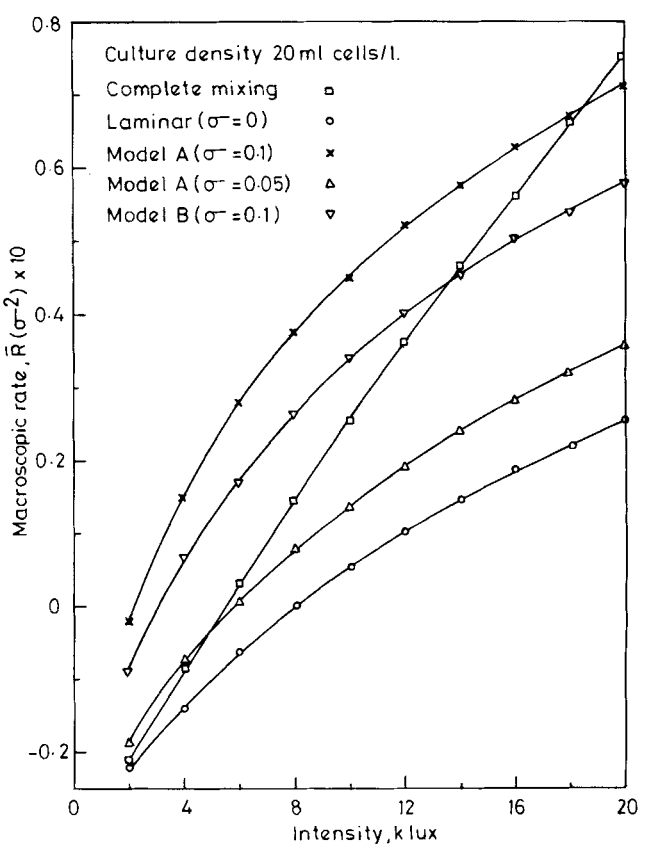

Fig. 7. Macroscopic rate as a function of light intensity.

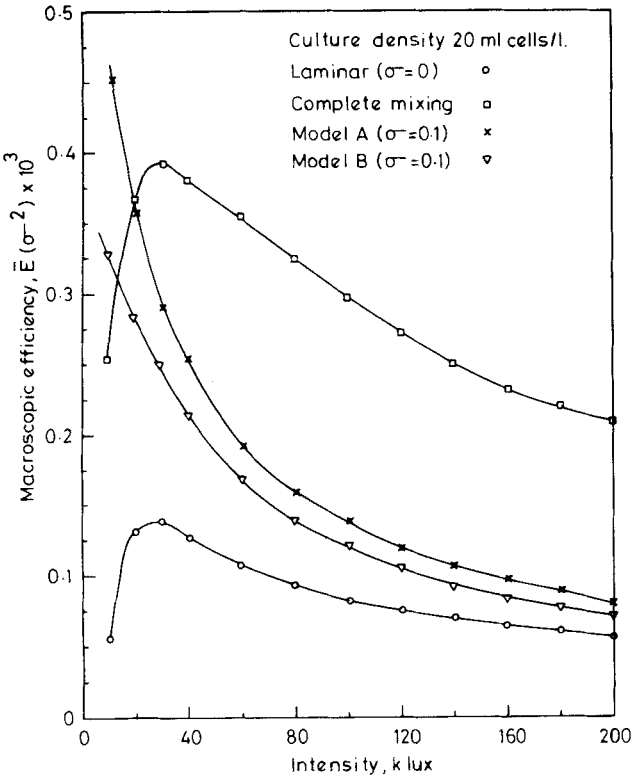

Fig. 8. Macroscopic efficiency as a function of light intensity.

surface and virtually complete darkness away from the surface.

Figure 6 shows the macroscopic photosynthetic rate plotted as a function of light intensity. Clearly, the rate is increased considerably for both models A and B, although well below that for complete mixing. Since experimental work has not ever produced such dramatic increases as

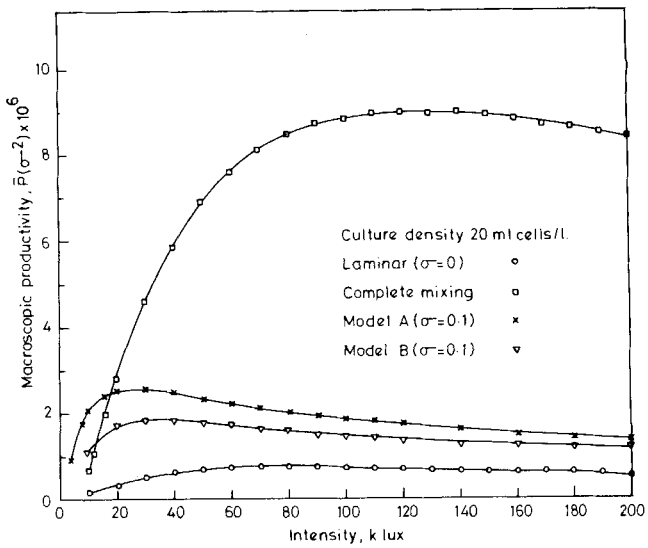

Fig. 9. Macroscopic productivity as a function of light intensity.

shown by the complete mixing model, it must be concluded that complete mixing cannot be approached even closely. For low light intensities, however, Figure 7 shows that models A and B predict a higher rate than the complete mixing model, which suggests that there may exist optimum degrees of turbulence for realizing the intermittency effects. This finding can be explained physically. In a dense culture, for low intensities, the bulk of the culture is in complete darkness, and only a thin layer is illuminated. On volume averaging, the light intensity may therefore become very small, thus lowering the rate even for the complete mixing model. The situation is not as bad for models A and B w.r.t. average light intensity; besides, intermittency effects are also realized. The rates are negative in Figure 7 because oxygen requirements for respiration exceed oxygen production for photosynthesis at low levels of illumination.

Figure 8 shows the macroscopic efficiency [Equation (26)] as a function of light intensity. An interesting aspect

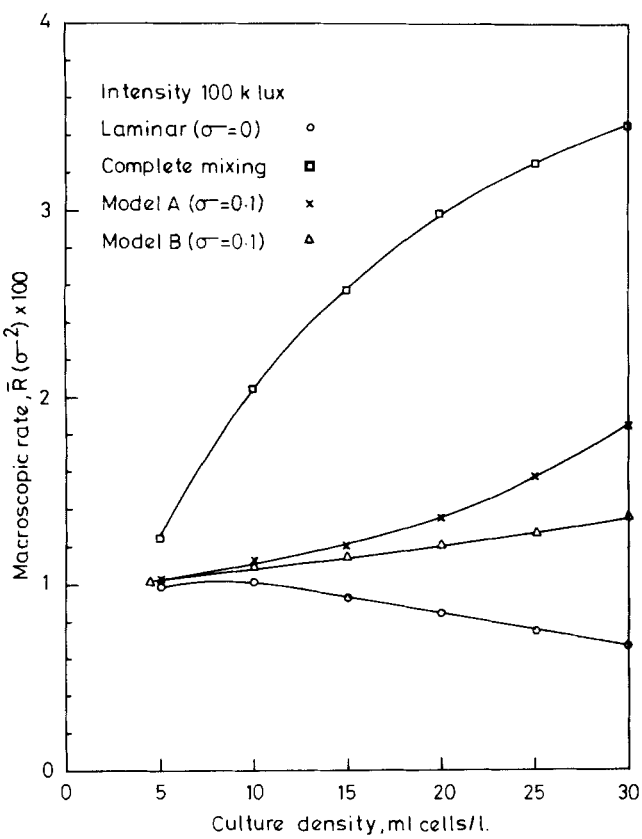

Fig. 10. Macroscopic rate as a function of culture density.

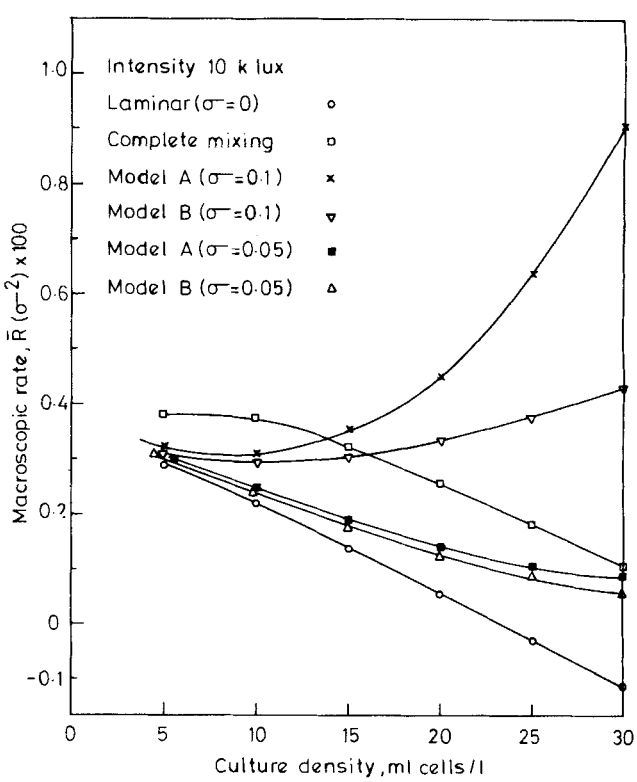

Fig. 11. Macroscopic rate as a function of culture density.

TABLE 2

k_1	k_2	k_s	k'_{ss}	C	ϵ	β	L
6.7×10^{10} g/mole × s	2.1×10^3 s^{-1}	4.6×10^{-6} $Lux^{-1}\,s^{-1}$	3.6×10^8 g/mole-s	7.0×10^{-5} mole/g	1.0×10^{-9} mole/g	0.8 l/cm-ml-cell	1 cm

of Figure 8 is that models A and B predict a monotonic decrease in efficiency with increasing illumination at low as well as high levels, unlike the complete mixing model which shows a point of maximum. This behavior is consistent with the experimental results of Miller et al. (1964). It is also evident from Figure 8 that at low light intensities, the macroscopic efficiencies predicted by models A and B are greater than those predicted by the complete mixing model. This result was speculated by Fredrickson et al. (1961).

The macroscopic productivity calculated from Equation (27) is plotted vs. light intensity in Figure 9. The curve shows a maximum, which shifts to smaller values of light intensity as culture density increases. Since the productivity accounts for both rate and efficiency, it seems desirable to use this function for optimal conditions.

Figures 10 and 11 display the macroscopic rate vs. culture density at two different light intensities. From Figure 11, it is obvious that at low intensities and high culture densities, the level of turbulence becomes extremely critical.

While models A and B have produced very useful information indicating that turbulence may be an asset for improving photosynthesis, their drawback lies in their idealizations. We consider below more realistic models for the random algal motion. The first of those, which will be called model 1, overcomes the objection to model A in that Equations (8) and (10) are inconsistent.

Model 1

The first obvious remedy is to assume that v_z' is white noise so that $Z'(t)$ becomes an autocorrelated process.

Thus, we assume for model 1 that $Z'(t)$ is a stochastic process with the properties

$$E[Z'(t)] = 0, \quad E[Z'(t)Z'(t+\tau)] = \sigma_z^2\, e^{-k\tau} \quad (28)$$

where σ_z^2 is the variance of Z'. This is the same as postulating that Z' satisfies the differential equation

$$\frac{dZ'}{dt} = -kZ' + \sigma k\, \xi(t) \quad (29)$$

with $\sigma^2 = 2\sigma_z^2/k$.

We use Tamiya's rate mechanism for photosynthesis incorporating Beer's law for the distribution of light intensity in the channel:

$$\frac{d}{dt}(S') = k_s I_o \exp\{-\beta[\overline{Z} + \xi(t)]\}\{C - [S']\} - k_1[S'] - k_1[S']\{\epsilon - [E_2]\} - 2\,k_{ss}[S']^2 \quad (30)$$

$$\frac{d}{dt}[E_2] = k_1[S']\{\epsilon - [E_2]\} - k_2[E_2] \quad (31)$$

The simultaneous solution of Equations (29), (30), and (31) subject to initial conditions is required to realize the predictions of model 1. The Fokker-Planck equation may be readily identified for the multivariate probability density for the processes in the above equations. However, the solution of this equation is exceedingly difficult so that we resort to a direct numerical solution of Equations (29), (30), and (31) by an algorithm due to Rao et al. (1974*b*). The details of the computation are present elsewhere (Sheth, 1974). Briefly, the calculation involves evaluation of sample paths of the algal motion (for every fixed $\overline{Z}$) by simulation, which consists of generating Gaussian random variables. Finer step sizes are required for higher light intensities and larger values of the variance parameter σ. For the parameters of the simulation (shown in Table 2), step sizes range from 0.0001 to 0.0002 s. The total time of any single simulation must be sufficiently long so that statistical quantities become time invariant, but not so long that accumulated errors become intolerable.

Figure 12 shows the mean microscopic rate as a function of time. Steady state may be seen to be achieved rapidly, and for the parameter values in the figure, the enhancement in the photosynthetic rate is evident. The number of sample paths must be large enough to provide for sufficient accuracy with which the averages are computed. Since the moments achieve a steady state, statistical averaging (by multiple simulations) may be replaced by time averaging, thus saving computational effort.

The microscopic rate is computed by simulation at each value of $\overline{Z}$. The macroscopic rate requires calculation for

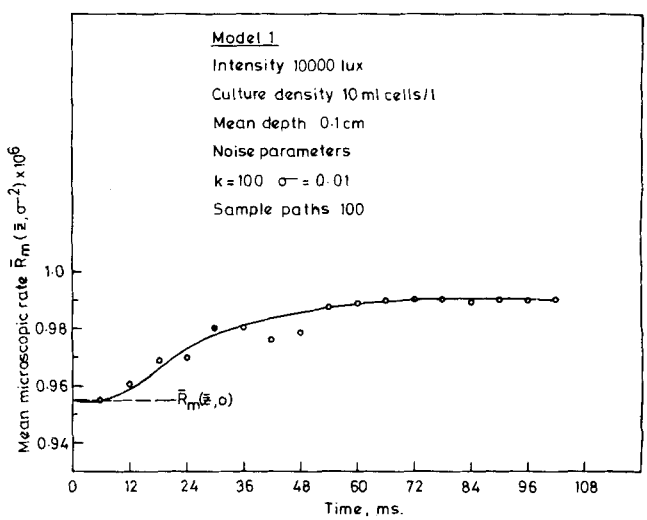

Fig. 12. Mean microscopic rate versus time: approach to steady state.

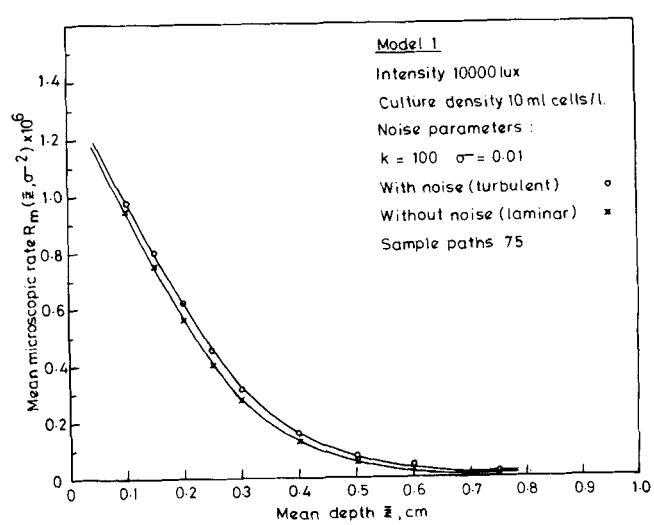

Fig. 13. Mean microscopic rate as a function of depth.

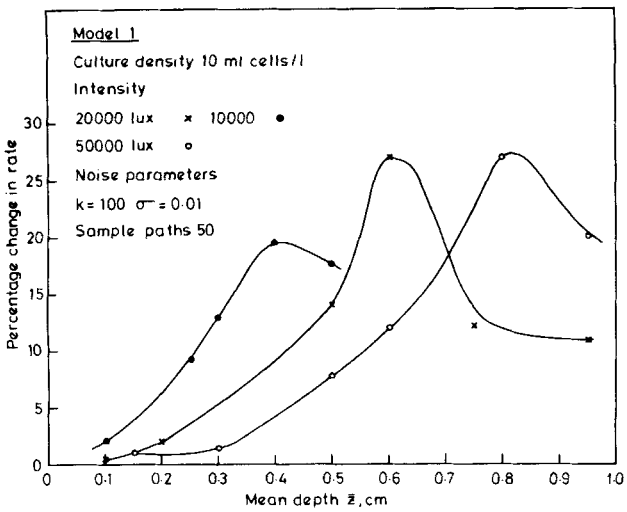

Fig. 14. P.C. changes in microscopic rate as a function of depth.

TABLE 3

N_{Re}	U_c cm/s	T_L s	$\sqrt{\overline{v_z^2}}$, cm/s
10^4	100	1.5×10^{-2}	3.00
1.25×10^4	125	1.1×10^{-2}	3.75
1.60×10^4	160	0.835×10^{-2}	4.80
2.0×10^4	200	0.64×10^{-2}	6.00
2.5×10^4	250	0.455×10^{-2}	7.50

different values of $\overline{Z}$ and integration numerically over the channel width. This was not done because of excessive computation times.* Instead, the microscopic rates were computed over widely varying values of $\overline{Z}$ from which the behavior of the macroscopic rate could be inferred. Figure 13 shows the results of such calculations from which the macroscopic rate can be seen to have been enhanced by turbulence. In Figure 14, the percent change in the microscopic rate over that for stagnant or laminar flow is plotted for different light intensities as a function of depth. The curves show a maximum shifting towards the deeper ends with increasing light intensity. It is clear that mixing near the surface is not of value, but for cells near the center, mixing produces substantial increase in photosynthetic rates. In deeper regions, where mixing is not sufficient to transport the cells into high intensity regions, the increase in rate drops off. From this behavior it is evident that for certain critical values of I_o, the level of turbulence may become extremely critical.

Model 2

Although model 1 is an improvement over models A and B, it does not use any available hydrodynamic information about channel flow. We now consider a model 2, which is exact only for homogeneous turbulence and relates parameters of the model to experimental data. The basis for the model is offered by Taylor's theory of diffusion (Taylor, 1936). It is readily shown that for a process $Z(t)$ in Equation (8) the autocorrelation function defined by

$$\overline{Z^2(t)} = \lim_{T\to\infty} \frac{1}{T}\int_o^T Z^2(t+\tau)\, d\tau \qquad (32)$$

is given by

$$\overline{Z^2(t)} = \int_o^t dt' \int_o^t dt'' \, \overline{v_z(t_o+t')v_z(t_o+t'')} \qquad (33)$$

* Calculations were performed on an IBM-7044. Computations of this kind can be performed readily on more modern computers.

The Lagrangian correlation coefficient is defined as

$$g_L(\tau) = \frac{\overline{v_z(t)v_z(t+\tau)}}{\overline{v_z^2}} \qquad (34)$$

By an elementary transformation, Equation (33) can be modified to accommodate (34) and to obtain

$$\overline{Z^2(t)} = 2\,\overline{v_z^2}\int_o^t dt' \int_o^{t'} d\tau\, g_L(\tau) \qquad (35)$$

which was obtained by Taylor (1936). Although the Lagrangian correlation is unknown, it has been customary to assume that $g_L(\tau)$ has the form

$$g_L(\tau) = e^{-\tau/T_L} \qquad (36)$$

where T_L is the Lagrangian time scale defined by

$$T_L = \int_o^\infty g_L(\tau)\, d\tau \qquad (37)$$

Using (36) in (35), we obtain

$$\overline{Z^2}(t) = 2\overline{v_z^2}\, T_L^2 \left[\frac{t}{T_L} - (1 - e^{-t/T_L})\right] \qquad (38)$$

The eddy diffusion coefficient is defined as

$$D = \frac{\overline{Z^2(t)}}{2t} \qquad (39)$$

so that for times large with respect to the time scale T_L, that is, $\frac{t}{T_L} << 1$, we have

$$D = \overline{v_z^2}\, T_L \qquad (40)$$

Equation (40) represents the means to use experimental information on measurements of $\overline{v_z^2}$ (which is the same as the turbulence intensity $\overline{v_z'^2}$, since $\bar{v}_z = 0$) and the eddy diffusion coefficient D to get T_L. Flint et al. (1960) have experimentally measured D for a point source turbulent diffusion in a pipe, which will be used in our calculations. They have presented a correlation for D as a function of Reynolds number. Laufer (1951) has measured $\overline{v_z^2}$ for turbulent flow in a channel, which together with measurements of D can be used in Equation (40) to calculate T_L. Thus, a reasonably realistic description of algal motion is at hand.

In order that (34) and (36) hold, we need only postulate that the velocity fluctuation v_z' satisfy the differential equation

$$\frac{dv_z'}{dt} = -\frac{1}{T_L}v_z' + \sqrt{\frac{2}{T_L}\overline{v_z^2}}\,\xi(t) \qquad (41)$$

Model 2 is therefore mathematically represented by the simultaneous differential Equations (41), (5), (30), and (31), which are to be solved subject to initial conditions. Again, the algorithm of Rao et al. (1974) was used to obtain sample pathwise solutions from which average values of microscopic rates are obtained. Table 3 shows the calculated values of T_L, U_c, and $\overline{v_z^2}$ for different Reynold's numbers (based on channel width) which were used in the simulation.

The percent increase in microscopic rate is plotted vs. Reynold's number for two different mean depths in Figures 15 and 16. The decrease in rate in Figure 15 reinforces earlier conclusions that mixing near the surface can be a disadvantage, especially at higher light inten-

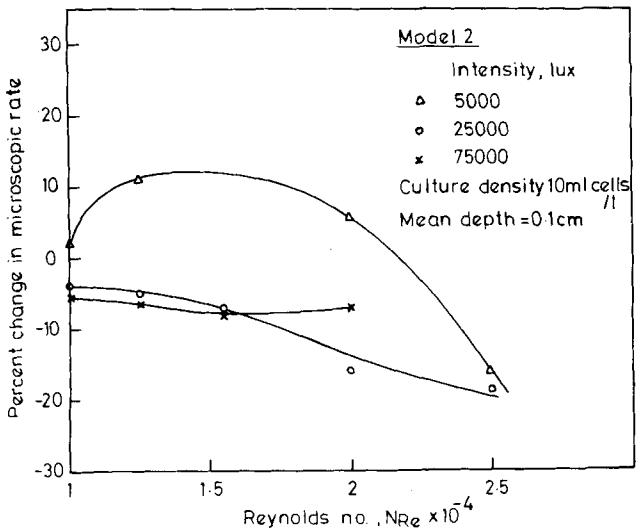

Fig. 15. Percent change in microscopic rate as a function of Reynolds number.

sities. Further down into the channel noticeable increase in photosynthetic rate may be observed from Figure 16. At the lower light intensity, an optimum degree of turbulence is evident, although it may vary with mean depth. Figure 17 shows the effect of light intensity at a fixed Reynolds number and mean depth on the percent increase in microscopic rate. Substantial increase may be observed at lower light intensities. In Figure 18 the increase in microscopic rate over most of the depths in the channel indicates a net increase in the macroscopic rate. Unfortunately, since computational facilities were constrained to a second-generation computer, no calculations could be made on macroscopic rates and efficiency of energy utilization or productivities.

CONCLUSIONS

From the different stochastic models of channel flow presented here, we can conclude that turbulent action in a channel improves the rate and efficiency of photosynthesis. The extent of improvement critically depends on the light intensity, culture density, and the degree of turbulence. An interesting aspect of the calculations is that mixing produces substantial improvements in microscopic rate in certain locations, but not in others. This is a useful guide to the strategic location of turbulence promoting devices such as wire baffles that could conceivably produce even

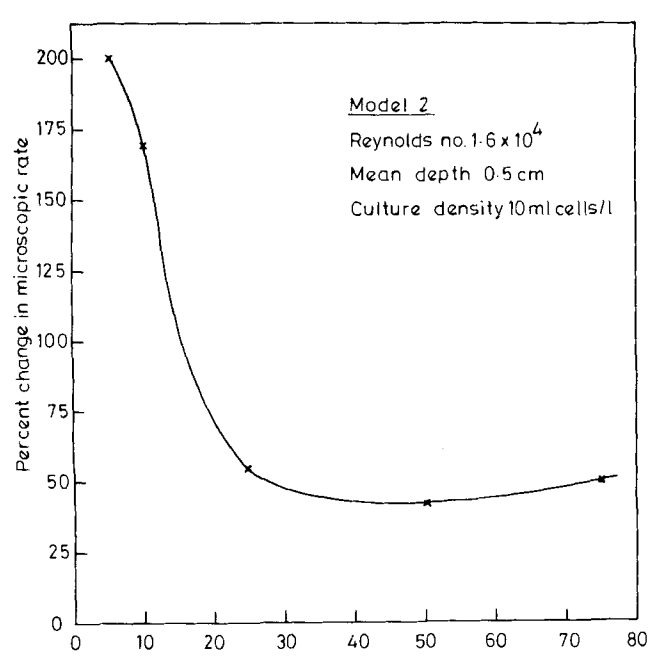

Fig. 17. Effect of light intensity on microscopic rates.

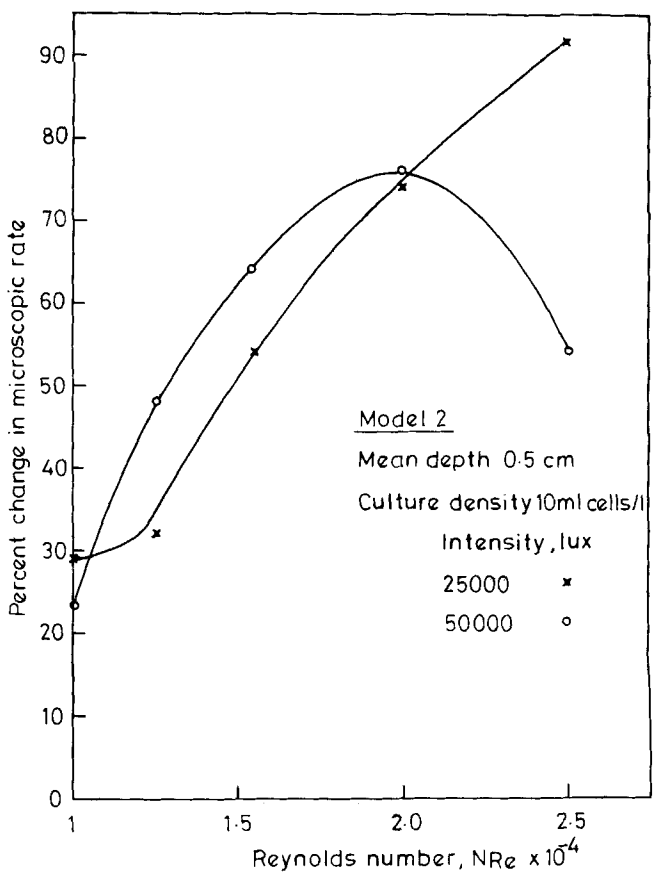

Fig. 16. Percent change in microscopic rate as a function of Reynolds number.

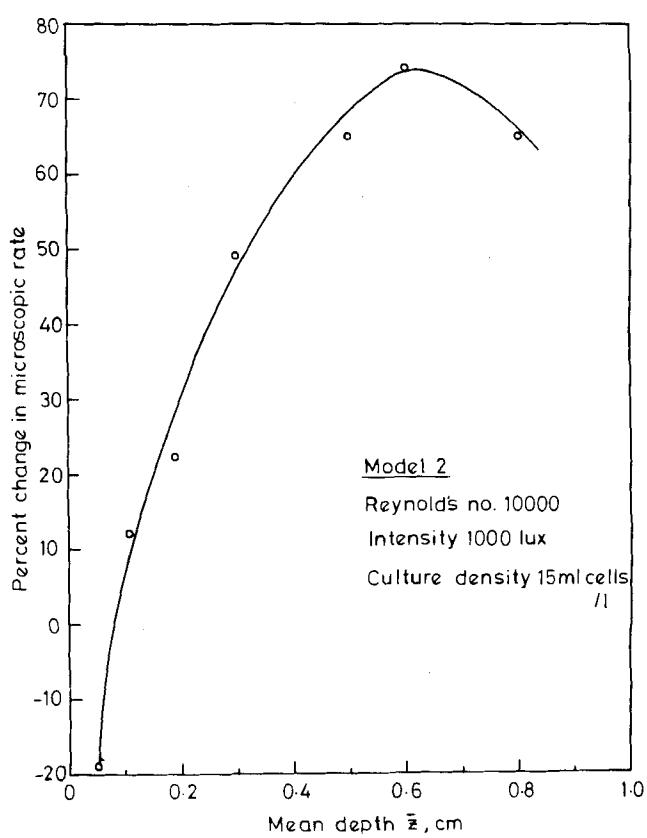

Fig. 18. Percent change in microscopic rate as a function of depth.

greater improvements in yields. On the basis of the results presented here, it would seem worthwhile to investigate cultivation of mass cultures of algae in open channels exposed to sunlight with a view to efficient utilization of solar energy.

Since photochemical reactions, in general, possess features similar to those of photosynthesis, the methodology presented in this paper would be applicable to these situations also.

NOTATION

C = constant in Tamiya rate mechanism
D = eddy dispersion coefficient
D_1 = variance in Equation (14)
E = enzyme, also, statistical expectation, efficiency
g_L = Lagrangian correlation coefficient
h = Planck constant
I = light intensity
k = rate constant, also, constant in Equation (28)
L = channel depth
M_x = mean of x
P = productivity
$\overline{R}_m$ = mean microscopic rate of photosynthesis
$\overline{R}$ = macroscopic photosynthetic rate
$\overline{S}$ = coefficient of variation of photosynthetic rate
t = time
U_c = mean velocity at the center of channel
W = Wiener process, W_x, second moment of x
Z = position of algal cell
$\overline{Z}$ = mean position of cell

Greek Letters

β = Beer's law coefficient
δ = Dirac delta function
ϵ = constant in Tamiya rate mechanism
ν = frequency of light
ρ = culture density
σ = standard deviation
τ = time increment in autocorrelation function

LITERATURE CITED

Flint, D. L., H. Kada, and T. J. Hanratti, "Point Source Turbulent Diffusion in a Pipe," *AIChE J.*, **6**, 325 (1960).

Fredrickson, A. G., A. H. Brown, R. L. Miller, and H. M. Tsuchiya, "Optimum Conditions for Photosynthesis in Optically Dense Cultures," *J. Am. Rocket Soc.*, **31**, 1429 (1961).

Fredrickson, A. G., and H. M. Tsuchiya, "Prediction and Measurement of Photosynthetic productivity," Proceedings of the IBP/PP Technical Meeting, Trebon (Sept., 1969), Wogeningen-The Netherlands (1970).

Gordon, A., "A Simulation Study of Flashing Light Effect in Algal Photosynthesis," M.S. thesis, Univ. Minn., Minneapolis (1972).

Kok, B., in *Algal Cultures from Laboratory to Pilot Plant*, J. S. Burlew, ed., Carnegie Institution of Washington, Washington, D. C. (1953).

Laufer, J., "Investigation of Turbulent Flow in a Two-Dimensional Channel," *NACA Technical Rept. 1053* (1951).

Lumry, R., and J. S. Rieske, "Mechanism of the Photochemical Activity of Isolated Chloroplasts. V. Interpretation of the Rate Parameters," *Plant Physiol.*, **34**, 301 (1959).

Miller, R. L., A. G. Fredrickson, A. G. Brown, and H. M. Tsuchiya, "Hydromechanical Method to increase Efficiency of Algal Photosynthesis," *Ind. Eng. Chem. Process Design Develop.*, **3**, 134 (1964).

Mortensen, R. E., "Mathematical Problems of Modeling of Stochastic Nonlinear Synamic Systems," *J. Stat. Phys.*, **1**, 271 (1969).

Pell, T. M., and R. Aris, "Some Problems in Chemical Reactor Analysis with Stochastic Features," *Ind. Eng. Chem. Fundamentals*, **8**, 339 (1969).

Powell, C. K., J. B. Chaddock, and A. J. R. Dixon, "The Motion of Algae in Turbulent Flow," *Biotech. Bioeng.*, **7**, 245 (1965).

Rao, N. J., D. Ramkrishna, and J. D. Borwanker, "Nonlinear Stochastic Simulation of Stirred Tank Reactors," *Chem. Eng. Sci.*, **29**, 1193 (1974, 1974*a*).

———, "Numerical Solution of Ito Integral Equations," *S.I.A.M. J. Control*, **12**, 124 (1974, 1974*b*).

Sheth, M., "Stochastic Models for Photosynthesis by Algae in Turbulent Flows," M. Tech. thesis dissertation, Indian Institute of Technology, Kanpur, India (1974).

Tamiya, H., "Analysis of Photosynthetic Mechanism by the Method of Intermittent Illumination, II. Theoretical Part.," *Stud. Tokugawa Inst.*, **6**, No. 2, 43 (1949).

Taylor, G. I., "Correlation Measurements in a Turbulent Flow Through a Pipe," *Proc. Roy. Soc. London*, **157A**, 537 (1936).

Warga, J., "Relaxed Variational Problems," *J. Math. Anal. Applications*, **4**, 111 (1961).

Wong, E., *Stochastic Processes in Information and Dynamical Systems*, McGraw-Hill, New York (1971).

Manuscript received March 7, 1977; revision received July 1, and accepted July 7, 1977.

Measurement of Zeolitic Diffusivities and Equilibrium Isotherms by Chromatography

The chromatographic method has been used to study the sorption and diffusion of methane, ethane, propane, and cyclopropane in 5A molecular sieve. Both the equilibrium isotherms and the time constants for zeolitic diffusion, obtained from the chromatographic peaks, agree well with the values obtained previously by the gravimetric method, thus confirming the validity of the experimental technique. The results obtained in several previously reported chromatographic studies are reviewed, and it is shown that the apparent discrepancies between chromatographic and gravimetric data arise mainly from differences in the way in which the micropore diffusivity is defined. The relative advantages and disadvantages of the gravimetric and chromatographic methods are briefly considered.

DHANANJAI B. SHAH

and

DOUGLAS M. RUTHVEN

Department of Chemical Engineering
University of New Brunswick
Fredericton, N.B., Canada

SCOPE

The chromatographic method has been suggested as an alternative to the conventional gravimetric or volumetric methods for studying the kinetics and equilibrium of sorption in biporous adsorbents such as molecular sieves. However, there has been no detailed comparison between results obtained, under comparable conditions, by chroma-